The Statistical Severe Convective Risk Assessment Model

JOHN A. HART AND ARIEL E. COHEN

NOAA/NWS/NCEP/Storm Prediction Center, Norman, Oklahoma

(Manuscript received 29 December 2015, in final form 9 August 2016)

ABSTRACT

This study introduces a system that objectively assesses severe thunderstorm nowcast probabilities based on hourly mesoscale data across the contiguous United States during the period from 2006 to 2014. Previous studies have evaluated the diagnostic utility of parameters in characterizing severe thunderstorm environments. In contrast, the present study merges cloud-to-ground lightning flash data with both severe thunderstorm report and Storm Prediction Center Mesoscale Analysis system data to create lightning-conditioned prognostic probabilities for numerous parameters, thus incorporating null-severe cases. The resulting dataset and corresponding probabilities are called the Statistical Severe Convective Risk Assessment Model (SSCRAM), which incorporates a sample size of over 3.8 million 40-km grid boxes. A subset of five parameters of SSCRAM is investigated in the present study. This system shows that severe storm probabilities do not vary strongly across the range of values for buoyancy parameters compared to vertical shear parameters. The significant tornado parameter [where ''significant'' refers to tornadoes producing (Fujita scale) F2/(enhanced Fujita scale) EF2 damage] exhibits considerable skill at identifying downstream tornado events, with higher conditional probabilities of occurrence at larger values, similar to effective storm-relative helicity, both findings being consistent with previous studies. Meanwhile, lifting condensation level heights are associated with conditional probabilities that vary little within an optimal range of values for tornado occurrence, yielding less skill in quantifying tornado potential using this parameter compared to effective storm-relative helicity. The systematic assessment of probabilities using convective environmental information could have applications in present-day operational forecasting duties and the upcoming warn-on-forecast initiatives.

1. Introduction

Advances in weather forecasting have accelerated during the last several decades owing to the development of increasingly sophisticated science and technology—including the improved assimilation of atmospheric observations, fundamental developments in numerical weather prediction, increasing computational resources, and the continued development of conceptual models bridging together observational and modeling realms (e.g., Schwartz et al. 2014; Bryan et al. 2003; Johns and Doswell 1992; Galway 1992; Burgess and Lemon 1990; Lewis 1989; Scofield and Purdom 1986). The evolution of severe thunderstorm forecasting is no different, and recent advances in convection-allowing model guidance have proven to be beneficial in providing more accurate and precise forecasts (e.g., Done et al. 2004; Kain et al. 2003; Weisman et al. 2008). Also, recent advances in numerical weather prediction have permitted the development of the more frequently updating mesoscale Rapid Update Cycle (RUC) and Rapid Refresh model (RAP), which run hourly and ingest the most recently observed data. The purpose of the present study is to extend these advances forward, by developing a systematic procedure to evaluate the probability of future severe weather occurrence.

Severe thunderstorm occurrences are highly dependent on a wide array of subgrid-scale processes that numerical models currently cannot explicitly resolve (e.g., microphysical processes and turbulence within the planetary boundary layer), and the convective interactions that take place greatly modulate the severe weather risk (Bryan et al. 2003). For these reasons, products from high-resolution models are limited in their usefulness as a tool in forecasting severe convective storms. However, early forecast errors propagate well downstream spatiotemporally, particularly in weak-forcing-for-ascent regimes, and can render such model

Corresponding author address: John Hart, Storm Prediction Center, 120 David L. Boren Blvd., Norman, OK 73072.
E-mail: john.hart@noaa.gov

DOI: 10.1175/WAF-D-16-0004.1

output inaccurate (e.g., Jankov and Gallus 2004). Given the current limitations of mesoscale and convection-allowing models for the prediction of impactful severe storms, additional observationally based approaches are still needed at short temporal ranges (a couple of hours into the future). These limitations serve as the motivation for this work, which provides a systematic approach to quantifying short-term severe thunderstorm potential based upon observationally influenced meteorological datasets—specifically considering the potential for a thunderstorm in a given environment to subsequently produce severe weather over the next couple of hours.

Forecasters make use of longstanding procedures that have stood the test of time, including the assessment of meteorological parameters, while also considering meteorological patterns as compared to longer-term, climatological patterns (Johns and Doswell 1992). The present study focuses on the first of these elements (i.e., the evaluation of meteorological parameters) as it pertains to formulating forecasts of severe weather conditions based upon present-state parameters. Doswell and Schultz (2006) challenge the notion of using diagnostic parameters as the basis for prognostic expectations regarding forecasted severe storm occurrences. They associate complexities in atmospheric processes with the inability to accurately draw conclusions about the future state of the atmosphere from initial conditions described by a single parameter. However, they do offer a solution to this problem, whereby both event occurrences and null cases (nonevent occurrences) are combined to determine the relative frequency of event occurrences for specific values of the parameter, which translates to a probability of event occurrence. This highlights the aim of the present study: to develop a systematic procedure for applying this solution, by which the probability of severe weather occurrence in the future is linked to a parameter value or set of parameter values. This systematic procedure serves as the foundation of the Statistical Severe Convective Risk Assessment Model (SSCRAM).

The comparisons of meteorological parameters (e.g., measures of buoyancy and vertical shear) to past severe weather occurrences provide a background for anticipating severe storm risk based on initial environmental information (e.g., Rasmussen and Blanchard 1998; Thompson et al. 2003, 2007; Craven and Brooks 2004). These studies provide background for forecasters to anticipate future severe weather occurrences based on past ones using meteorological parameter values. However, the process of going about linking particular parameter values with severe storm occurrence does not account for the full severe storm probabilistic spectrum corresponding to a particular variable. For example, not every environment characterized by a certain parameter value often linked to severe storms actually results in severe storm occurrence. This motivates the need to incorporate a null event database into our understanding of the propensity for certain parameter values to support a severe weather risk, specifically to quantify severe weather potential based on both occurrences and nonoccurrences of an event.

Specifically, the present study couples lightning data to near-storm environmental information in spatiotemporal proximity to the lightning, and then queries areas downstream of lightning into the future for severe storm occurrences. The environmental information is based on output from the Storm Prediction Center (SPC) mesoanalysis system. The combination of these various sources allows us to derive probabilistic distributions conditioned upon lightning occurrence for severe reports occurring downstream. This effectively translates to a method of quantifying severe storm probabilities in the future given a thunderstorm, based upon the near-storm environment. Ultimately, such probabilistic information would be most relevant within a couple of hours extending into the future. Later prospects for severe storms would be increasingly influenced by storm interactions and environmental temporal variability, limiting the utility of initial-time environmental information in describing the later severe storm risk. Thus, such work has direct applicability in the range of "warn-on-forecast" (Stensrud et al. 2009) and Forecasting a Continuum of Environmental Threats initiatives (Rothfusz et al. 2013).

2. Data and methods

a. *Design of SSCRAM*

The SSCRAM-based derivation of probabilistic distributions corresponding to severe thunderstorms (damaging winds, large hail, and tornadoes) is based on meteorological information from the SPC environmental database (Dean et al. 2006), which also includes National Lightning Detection Network cloud-to-ground (CG) lightning flash data. Specifically, this dataset provides hourly lightning flash counts and environmental conditions within every 40-km grid box across the contiguous United States. SSCRAM-derived probabilities are conditioned on CG lightning, such that downstream querying of severe thunderstorm reports stems from CG lightning occurrences. This conditionality is justified by the linkage between severe thunderstorms and CG lightning (e.g., Maier and Krider 1982; MacGorman et al. 1989). However, Nag et al. (2011), for instance, demonstrate that NLDN lightning data are associated with some error, including misestimates of peak current

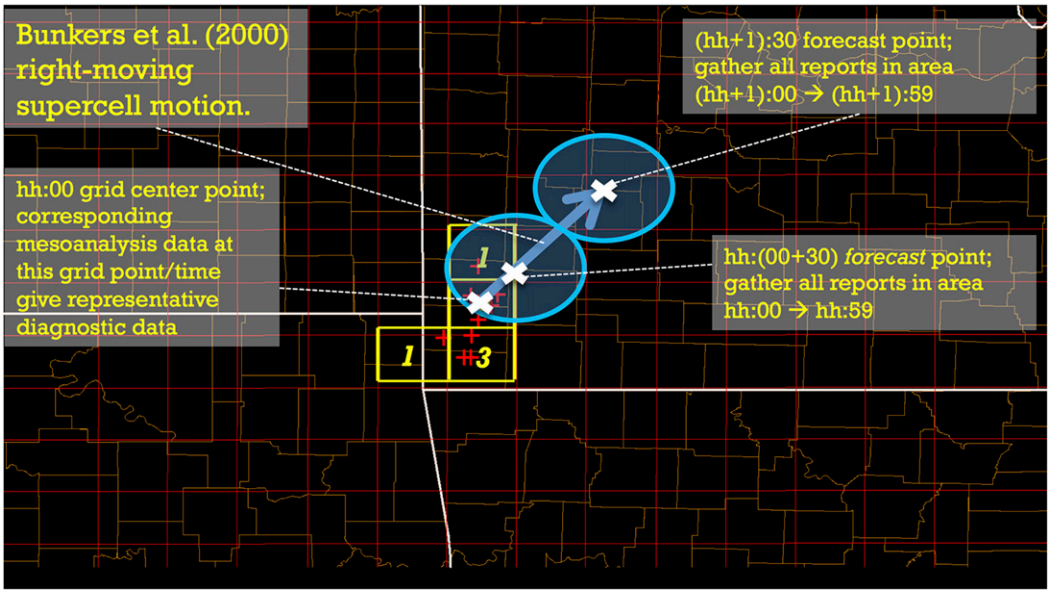

FIG. 1. Schematic demonstrating the process of ascertaining downstream severe storm reports from each lightning-associated grid box. This schematic depicts an example with CG lightning flashes that occurred within an hour denoted by hh and minutes denoted by mm (formulating the time hh:mm). Red plus signs (+) indicate every lightning strike that occurred in the hh:00–hh:59 time period. Yellow-outlined, lightning-containing, 40-km-wide grid boxes (numbered) are overlaid. White exes (x) indicate center points of the grid box at the initial time (hh:00) and future/downstream positions for analysis based upon the Bunkers et al. (2000) right-moving supercell motion with surrounding search circles (in blue) extending outward to 40 km. This represents a cumulative total of 2 h of severe storm report collection forward in time from the lightning-associated grid box by considering two different search zones centered on points extrapolated forward in space from the initial lightning-associated center grid point. Severe reports in each zone are restricted to those occurring within 30 min of the forward-extrapolated point. In this example, downstream search areas emanating from the grid box between those labeled 1 (to the north) and 3 (to the south), only, are considered for the illustration of this example.

and strike location. Regardless, NLDN CG lightning data are accepted as a primary source of lightning data in the operational meteorology community owing to their widespread availability and are the only archived lightning dataset in the SPC environmental database during the study period. While in-cloud lightning occurrences are not included in these archives, strong relationships do exist between total lightning and severe thunderstorm reports (e.g., Schultz et al. 2009, 2011, 2013). Since the present study does not incorporate in-cloud lightning data, it is possible that some grid boxes that are associated with thunderstorms are not included in the analysis (i.e., those that do not include CG lightning). This merely restricts the sample size of candidate environments for consideration of downstream severe storm reports to those associated with CG lightning strikes.

A schematic that highlights the approach to severe storm querying, emanating from a grid box containing CG lightning, in the SSCRAM system is provided in Fig. 1. Figure 1 illustrates the process of considering all severe storm reports occurring within 2 h into the future, within proximity to a forward trajectory from the center point of the grid box. Only one lightning strike is necessary to define a grid box as "lightning containing," as opposed to multiple CG strikes, effectively using the presence of any CG as a proxy for a thunderstorm contained within the grid box.

Output from the SPC mesoanalysis system (Bothwell et al. 2002) is used as the basis of characterizing near-storm environments for lightning-containing grid boxes. The mesoanalysis system combines surface observations with upper-air vertical profiles on a 40-km horizontal grid based upon the RUC from 1 January 2006 through 30 April 2012 and upon the RAP from 1 May 2012 through 2014. By associating lightning strikes with the mesoanalysis data, we establish near-storm environmental data for which we evaluate the corresponding severe thunderstorm report potential based on a search for severe thunderstorm reports. Numerous kinematic and thermodynamic parameters are available within the system, with many such parameters having been combined to generate composite parameters that characterize various aspects of the ongoing severe thunderstorm risk. Forecasters can use

such variables in tandem with an understanding of the convective mode to generate short-range expectations regarding the severe weather risk in a certain area.

As illustrated in Fig. 1, each lightning-containing grid box (as determined by gridded lightning data) represents a moving convective element that may or may not produce severe weather reports downstream (or even be sustained) and whose forward motion is estimated using the Bunkers et al. (2000) right-moving supercell motion technique. This technique is used in the present study to determine a focus area for possible severe storm reports given initial storm motion, as it is applicable to high-impact severe supercell storms that are responsible for a considerable percentage of severe weather (Trapp et al. 2005). Additional methods of estimating storm motion are presented in section 3, which provides further substantiation for the use of the Bunkers et al. (2000) technique in this study. The use of the Bunkers et al. (2014) technique for improving estimations of supercell motion based on pressure-weighted mean wind through a variable-layer depth dependent upon the base of the effective inflow layer and the most-unstable equilibrium-level height is not used in the present study. Given the error inherent to this motion technique (Bunkers et al. 2000), combined with the possibility of lightning-producing convection occurring with other convective modes, a radius of 40 km is applied as a search radius to query downstream severe storm reports. This radius is specifically chosen to match the grid length of the SPC Mesoanalysis dataset. Furthermore, this radius represents a displacement corresponding to severe storm motions during the evaluated temporal search intervals that would capture related reports in many instances. Specifically, for two search areas to be conjoined, a storm must be moving no faster than 80 km h^{-1} to ensure that the 2 h of downstream search invoke continuous area, which is in excess of mean storm speeds for supercells whose motions were studied by Edwards et al. (2002).

The accumulation of severe storm reports downstream of a lightning-strike-associated grid box, whose diagnostic environmental information is documented, directly links parameter values at a given location to the severe storm potential in the future. As such, no checks of downstream lightning occurrence are performed to evaluate the sustenance of a thunderstorm, as the goal of the present work is to make a nowcast of ongoing lightning-producing convection without the a priori assumption that lightning is sustained. An ''event'' corresponds to the occurrence of at least one severe thunderstorm report (severe hail, severe wind, or tornado report) within 2 h following initial grid-hour lightning occurrence within the downstream search area described previously and outlined in the shaded areas downstream of the initial-hour lightning-centered grid box illustrated in Fig. 1. If no report occurs within this search area, then a null event is documented. No distinction is made between reports occurring during the first versus second hours into the future and associated search areas. Because of the large variability of lightning frequency associated with severe and nonsevere thunderstorms, and the potential for multiple storms to affect individual grid boxes, no attempt is made in this study to distinguish between grid boxes containing more lightning. The presence or absence of lightning is used as the foundation for treating individual grid boxes as storms for reproducible, consistent analysis in this model.

While Fig. 1 provides an example of the analysis of severe reports corresponding to a single grid box, every lightning-containing grid box in the SSCRAM system database is also associated with respective downstream search areas. The example in Fig. 1 only demonstrates the one downstream extrapolation. Each grid box and the associated downstream search radii are considered independently of one another, prior to aggregating severe thunderstorm–linked and nonsevere thunderstorm–linked grid boxes for subsequent statistical analysis. Thus, lightning-associated grid boxes are not initially clustered together in the determination of downstream search radii. However, aggregation of environmental information and documentation of severe storm reports (or lack thereof) for each lightning-containing grid box permit the development of probabilistic distributions for future severe storm reports conditioned upon lightning. Based upon the design of SSCRAM, five variables (selected among numerous other options available in the SSCRAM database) are considered in this study to quantitatively evaluate probabilities of occurrence of severe thunderstorm events, including tornado events, in a retrospective manner. These five parameters (defined below) are specifically chosen to characterize the kinematic and thermodynamic environment of thunderstorms in evaluating their severe weather potential.

Some limitations to the SSCRAM system do exist. For example, this approach does not address differences between the environmental characteristics of the initial-hour lightning-strike-associated grid box and those of both the first- and second-hour search areas. This may not incorporate the effects of large scalar advection magnitudes and/or dynamically evolving weather systems that modulate vertical kinematic and thermodynamic profiles, rendering spatial and/or temporal variations in the environment. However, we chose to consider severe storm reports for only a short duration into the future (2 h) to mitigate the degree of spatiotemporal variability in environmental fields with the evolving convection.

Additionally, it is assumed that diagnostic parameters are homogeneous across the initial-hour grid box. This assumption could yield error for cases involving substantial within-grid-box parameter gradients, especially in cases where lightning only occurs on the edge of the grid box, though the relatively small size of the grid boxes is expected to largely overcome this error particularly given very large sample sizes involved in this study. One other source of error emanates from RUC and RAP analysis field errors above the surface, which will inherently extend to SSCRAM owing to the SPC Mesoscale Analysis System being model dependent.

Ultimately, any system will have limitations, but the short temporal constraint bolsters confidence that initial-hour environmental data are relevant in providing nowcasting utility for severe storm occurrence. Furthermore, the method of SSCRAM allows for an extremely large sample size, including around 3.8 million lightning-strike-associated grid boxes during the period from 2006 to 2014 to reduce the impact of individual outlier cases on the overall sample. SSCRAM's comprehensive scope allows for the examination of the climatology of various severe weather parameters, given the presence of CG lightning. With approximately 3.8 million data points, SSCRAM offers our best-to-date illustration of the longer-term distribution of various severe weather parameters. By determining the downstream relative frequencies of occurrence of severe wind, severe hail, and tornado reports over the large sample, we translate these quantities to probabilities of severe report occurrence for various ranges of parameter values corresponding to the lightning-associated grid box.

Subsequent discussion provides analysis of severe storm report probabilities corresponding to a subset of five variables for which SSCRAM yields severe storm probabilities: the effective-layer significant tornado parameter (STP), defined by Thompson et al. (2012); the lifting condensation level (LCL), based upon the lowest-100-mb mixed-layer parcel; the effective storm-relative helicity (SRH), defined by Thompson et al. (2007); effective bulk shear (Thompson et al. 2007); and convective available potential energy (CAPE). Some of these parameters will be discussed exclusively within the context of tornado forecasting. For example, tornado environments are accepted as being characterized by large SRH (e.g., Davies-Jones et al. 1990) and low LCL heights (e.g., Rasmussen and Blanchard 1998; Thompson et al. 2003). Observations from the Verifications of the Origins of Rotation in Tornadoes Experiment (VORTEX) suggest that greater relative humidity within the boundary layer, associated with lower cloud bases, is more conducive to minimizing the negative buoyancy within a supercell's rear-flank downdraft and its propensity to support tornado development (Markowski et al. 2002). Such environments facilitate the development of helical updrafts through the storm's ingestion of streamwise vorticity (measured by SRH) and do not produce particularly cold, downwardly buoyant outflow (Markowski et al. 2002).

b. *Statistical analysis procedure*

The SPC forecasts severe thunderstorm probabilities for individual hazards during the day-1 period: severe thunderstorm wind, severe hail, and tornadoes. As such, severe thunderstorm events will subsequently be discussed with a focus on probabilistic evaluation for individual hazards. Furthermore, tornado event intensity is stratified into two regimes, specifically 1) significant tornadoes [tornadoes producing (Fujita scale) F2/(enhanced Fujita scale) EF2 or greater damage] and 2) weak tornadoes (tornadoes producing F1/EF1 or lesser damage). This is done, as in the SPC convective outlooks and watches, in order to gauge the signal between two broader impact levels from tornadoes.

Two quantities are the focus of subsequent discussion, with plots provided corresponding to ranges of environmental parameters that represent typical orders of magnitude that forecasters consider in their use (e.g., bin size of 1 for STP): 1) conditional probability of a severe thunderstorm event and 2) relative frequency of occurrence of a severe thunderstorm. The first quantity is mathematically defined as follows:

$$(\text{conditional probability})_i = \frac{V_i}{N_i}, \tag{1}$$

where N represents the total number of lightning-containing initial-hour grid boxes (referred to as environs) within a certain indexed parameter range i and V represents the number of those grid boxes associated with downstream severe weather events (referred to as events). As an example, a conditional probability of 65% for a particular parameter range indicates that 65% of lightning-containing grid boxes associated with that parameter range are linked to downstream severe weather reports. The second quantity is mathematically defined as follows:

$$(\text{relative frequency})_i = \frac{V_i}{\sum_{k=1}^{k=x} V_k}, \tag{2}$$

such that the quantity V (i.e., within a specific indexed parameter range i) is compared to the total number of lightning-containing initial-hour grid boxes that associate

with severe reports *for any parameter range*. The latter element of comparison reflects a summation from the first parameter range with index 1 through all parameter ranges (i.e., to the parameter range with index x). Thus, the relative frequency is an indication of the proportion of severe weather environments associated with each parameter range. For example, a relative frequency of 43% for a particular parameter range indicates that 43% of severe weather–producing environments occur within that parameter range. This quantity does not distinguish between severe weather and nonsevere weather–producing environments, as a primary focus of this study is to provide forecasters with guidance on the frequency of severe weather occurrence, rather than the frequency of environmental occurrence.

One final quantity that is subsequently presented in limited scope uses the same nomenclature as that provided above:

$$(\text{exceedance probability})_i = \frac{\sum_{i=k}^{i=x} V_i}{\sum_{i=k}^{i=x} N_i}, \qquad (3)$$

where k represents the index of a parameter range for which an exceedance probability is computed. The exceedance probability is an indication of the probability of severe weather reports occurring downstream of lightning for any parameter values meeting or exceeding a particular threshold. Forecasters may use such integrated probabilities as a means of accounting for the uncertainty in exact parameter values by considering a range of such values for anticipating severe weather potential. A conditional probability, which is associated with a single parameter range, can be greater than, less than, or equal to the corresponding exceedance probability that incorporates multiple parameter ranges in both the numerator and denominator of its calculation. Formalized statistical testing has not been incorporated into this analysis for the purpose of illustrating the operationally and application-relevant portions of statistical tendencies. As an example, an exceedance probability of 8% for a particular parameter value indicates that 8% of lightning-containing grid boxes associated with that parameter value or any higher parameter value are linked to downstream severe weather reports.

3. Results and discussion

a. Statistical results and discussion for severe wind and severe hail

Conditional probabilities of severe wind events are found to steadily increase with greater most unstable CAPE (MUCAPE), while the majority of severe hail and wind events occur at MUCAPE below 3000 J kg^{-1} (Fig. 2). The interpretation of these results is that increasing MUCAPE shows a signal for greater conditional severe wind and hail risk, downstream of initial lightning occurrence, though very strong and extreme instability cases are rare in occurrence. Compared with MUCAPE, Fig. 3 illustrates somewhat greater utility of effective bulk shear as a conditional forecast parameter for severe wind and hail. Probabilities of severe wind and hail increase notably with increasing values of effective bulk shear, with relatively more substantial probabilities for severe wind (hail) events becoming evident for effective bulk shear magnitudes generally above 30–35 kt (40–45 kt, where 1 kt = 0.51 m s^{-1}).

Most-common ranges of effective bulk shear associated with severe wind events consistently decrease with increasing MUCAPE (Fig. 4a), as illustrated in Fig. 4, which stratifies the SSCRAM dataset based upon multiple MUCAPE constraints: at intervals of 1000 J kg^{-1}. This suggests that a larger proportion of the severe wind events in high-MUCAPE environments occur with weaker vertical shear, reflecting the rare nature for high buoyancy to overlap with large vertical wind shear in environments supporting severe winds. Furthermore, for most any effective bulk shear bin range, increasing MUCAPE corresponds to increasing conditional probabilities of severe winds (Fig. 4b).

The relationships between parameters such as MUCAPE and vertical shear and severe wind and hail build upon work performed by Schneider and Dean (2008), who illustrate relationships between measures of integrated buoyancy and vertical shear and occurrences of severe wind and hail for a 5-yr climatology for severe storm environments across the United States. Positive relationships between parameters representing buoyancy and vertical shear, and severe storm occurrences, are well documented through a large body of severe weather research. Doswell and Schultz (2006) and references therein provide a foundation for these relationships, while the present study builds upon this work in quantifying these relationships at a fine parameter resolution scale, while incorporating the effect of null cases.

b. Statistical results and discussion for tornadoes

Regarding tornadoes, conditional probabilities of tornado events (weak or significant) vary negligibly across the spectrum of MUCAPE, as plotted in Fig. 5. Most of the tornado events occur in weak-to-moderate buoyancy regimes, but the overall utility in MUCAPE for predicting tornadoes, alone, is quite limited.

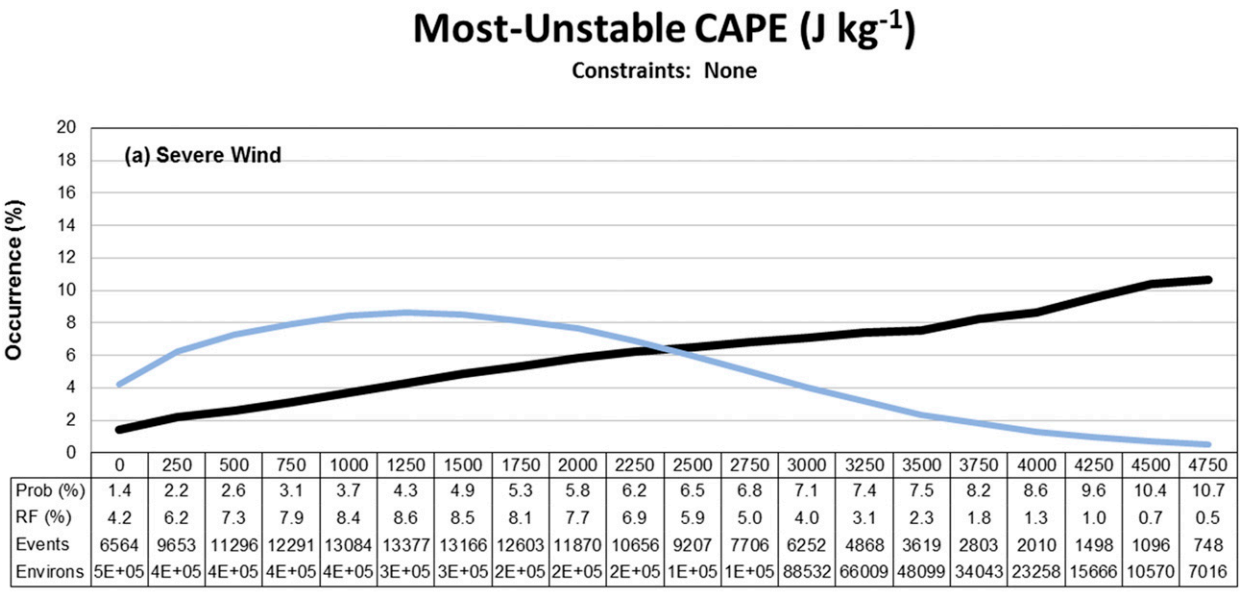

FIG. 2. (a) Conditional probability (Prob) of downstream severe wind occurring given a lightning strike within various ranges of MUCAPE values (in black), and the RF of severe wind–producing environments occurring within various ranges of MUCAPE values (in blue). Beneath the plot, the Prob and RF values corresponding to each bin are listed, along with the corresponding number of grid boxes associated with the reported downstream severe wind (events), and the number of grid boxes merely meeting the constraints (environs). For each parameter-range bin, Prob is equivalent to the events value divided by the environs value, whereas RF is equivalent to the events value divided by the sum of the events values over all parameter-range bins. Neither Prob nor RF values are provided for parameter-bin ranges with environs values of below 25. The value of MUCAPE corresponding to each bin range, listed immediately below the *x* axis, represents the minimum value of that range. (b) As in (a), but for severe hail events.

In contrast to MUCAPE, Fig. 6 shows that effective bulk shear exhibits increasing probabilities with increasing shear values for weak and significant tornadoes, with more frequent occurrence becoming evident for effective bulk shear magnitudes above 30 and 45 kt, respectively. This is consistent with some of the aforementioned work from Schneider and Dean (2008), who highlight the relationship between deep-layer shear and supercell thunderstorm development through their environmental parameter climatology, and the relationship between significant tornadoes and stronger deep shear is particularly evident in their work. In contrast, and entirely consistent with the present study, they find a much dampened dependence on buoyancy for tornadoes. In fact, they discourage using a minimum threshold of CAPE to assess significant tornado potential.

Figure 6b illustrates a notable decrease in conditional probabilities of significant tornadoes for effective bulk shear magnitudes of at least 80 kt. It is possible that

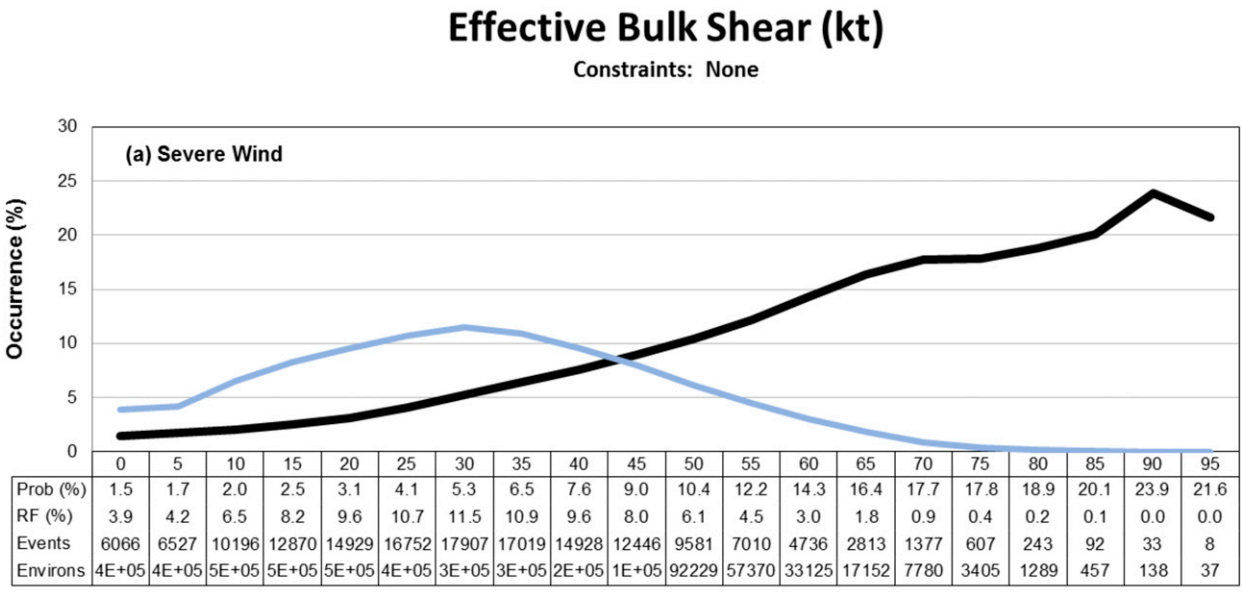

FIG. 3. Prob (black) and RF (blue) plots for effective bulk shear corresponding to (a) severe wind events and (b) severe hail events. The plotting and labeling process follows Fig. 2.

particularly fast storm motions in such environments could result in the underrepresentation of severe storm reports given the aforementioned design of SSCRAM, although the search for nonspeculative physical explanations for this tendency would be of particular interest in possible future research that could investigate sensitivities of the SSCRAM design. Furthermore, this decrease in conditional probabilities may reflect the small sample sizes of significant tornadoes occurring at such large values of effective bulk shear, and the small sample sizes of lightning-containing grid boxes characterized by these large effective bulk shear values.

Large proportions of both weak and significant tornado environments occur in association with low values of STP, as illustrated in Fig. 7, with proportions trailing off with increasing values of STP. In association with downstream-tornado-linked grid boxes featuring STP less than 1, 60.7% and 37.2% of those boxes verify with weak and significant tornadoes, respectively. There are some possible explanations for this finding: 1) STP is set to zero when effective bulk shear is below 12.5 m s^{-1} (24 kt) (Thompson et al. 2012); 2) the STP component that includes effective bulk shear is normalized by 20 m s^{-1} (39 kt) (Thompson et al. 2012), such that smaller values of effective bulk shear contribute to relative reductions in STP; and 3) the SPC Mesoscale Analysis System may not accurately represent the environment in which the tornadic storms are occurring.

With Fig. 6a (Fig. 6b) indicating just under half of all cases that verify with a weak (significant) tornado occur

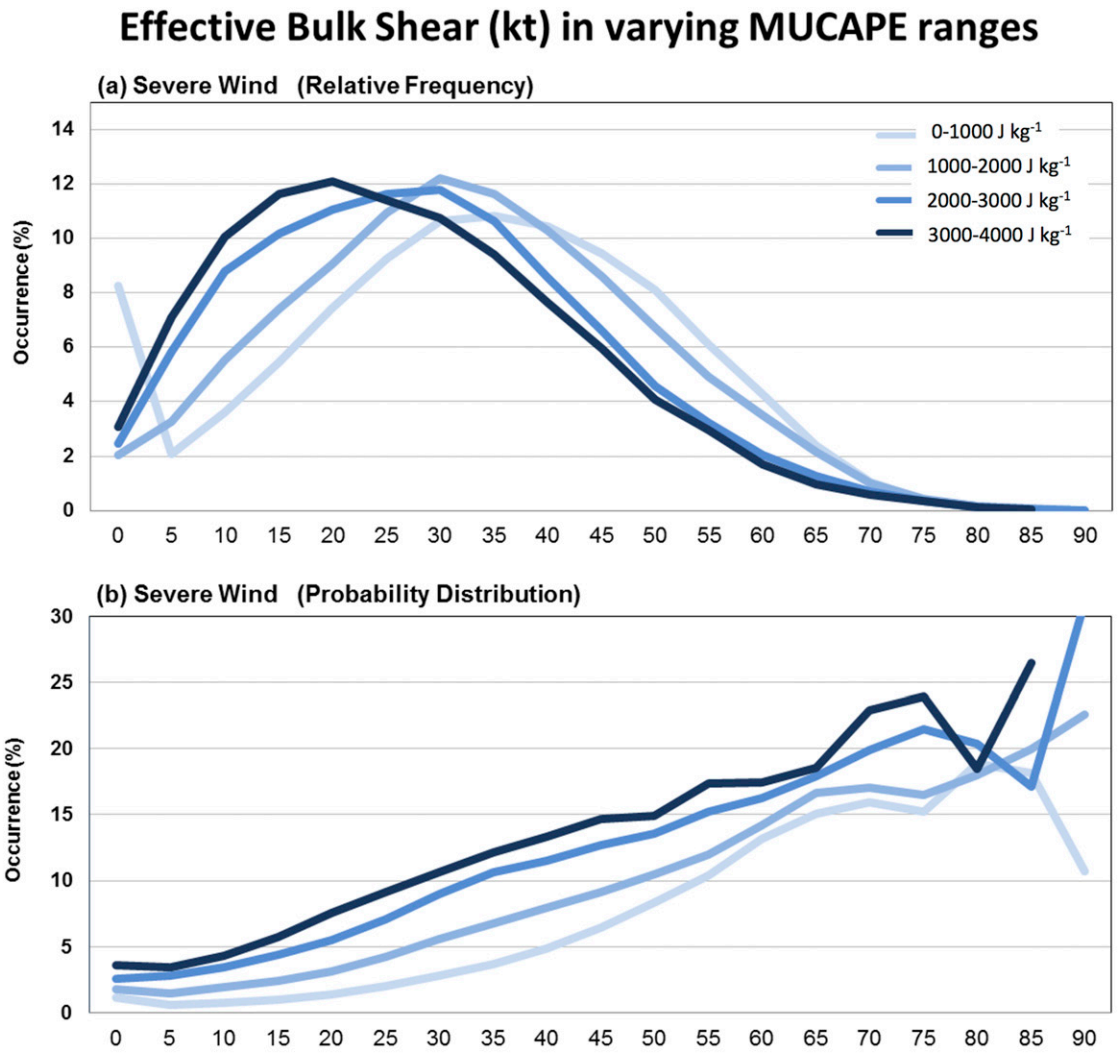

	0	5	10	15	20	25	30	35	40	45	50	55	60	65	70	75	80	85	90
Events (0-1000 J/kg)	3291	833	1437	2180	2968	3685	4234	4320	4163	3766	3221	2434	1693	955	424	156	71	20	3
Environs (0-1000 J/kg)	289821	142410	196977	216801	208677	183838	151044	116130	85353	58682	38642	23324	12883	6341	2655	1022	376	110	28
Events (1000-2000 J/kg)	1076	1703	2883	3880	4736	5711	6380	6074	5384	4499	3516	2579	1825	1122	531	231	92	40	14
Environs (1000-2000 J/kg)	60908	114386	151050	158653	151921	134800	113550	89388	67731	49393	33477	21520	12847	6722	3109	1399	511	200	62
Events (2000-3000 J/kg)	974	2311	3477	4021	4358	4597	4656	4199	3379	2607	1808	1275	812	502	277	136	55	18	9
Environs (2000-3000 J/kg)	37700	83130	100149	92093	78841	64529	51990	39474	29372	20500	13338	8359	4996	2806	1394	634	270	105	29
Events (3000-4000 J/kg)	539	1249	1762	2038	2118	2002	1887	1651	1341	1045	717	521	301	172	105	63	19	9	
Environs (3000-4000 J/kg)	14975	35827	40684	35569	27946	21934	17774	13556	10049	7135	4802	3004	1723	926	459	263	103	34	

FIG. 4. (a) RF and (b) Prob plots corresponding to effective bulk shear for severe wind–producing environments within four ranges of MUCAPE that are color coded based on different levels of blue shading. For each bin of effective bulk shear magnitudes, sample sizes corresponding to events and environs are provided beneath the *x* axis for each range of MUCAPE values (listed in parentheses).

in association with effective bulk shear below 45 kt (55 kt), it is well rationalized that most tornado events are associated with relatively lower values of STP, as shown by the relative frequency (RF) curves in Fig. 7a (Fig. 7b). These proportions (RF curves) decay nearly exponentially with increasing values of STP, also indicating the relative dearth of tornadoes occurring at high STP values.

Alternatively, conditional probabilities of both weak and significant tornado events increase with increasing STP values, reaching values around 10% and 20% for STP values in the 10–11 range bin for weak and

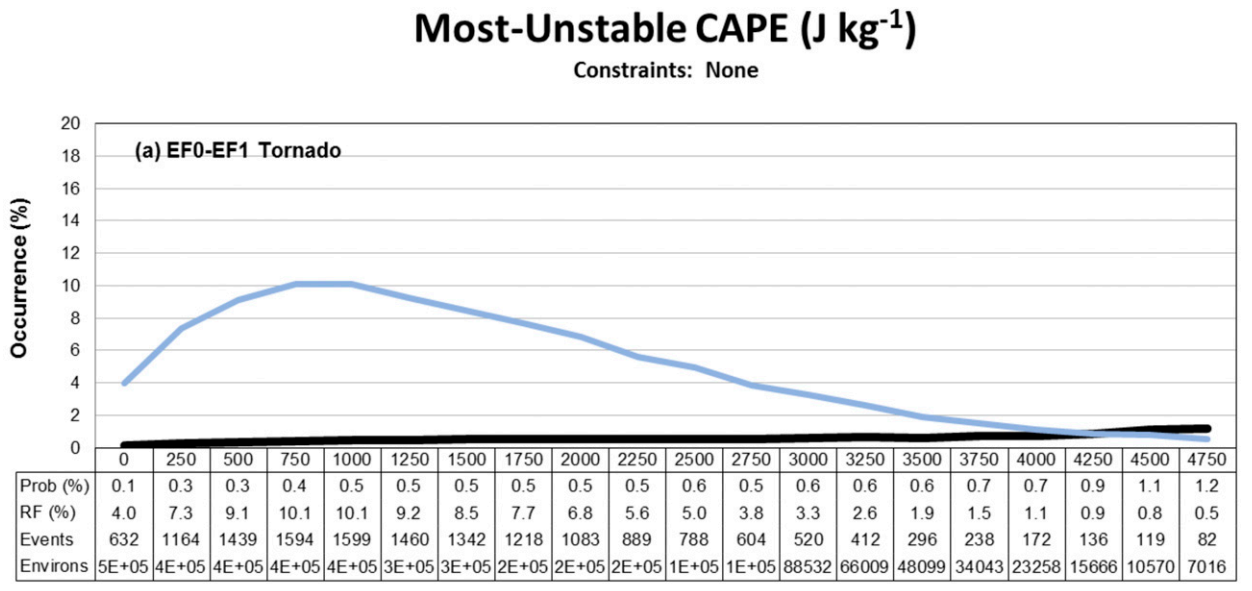

FIG. 5. The Prob (black) and RF (blue) plots for MUCAPE corresponding to (a) weak and (b) significant tornado events. The plotting and labeling process follows Fig. 2.

significant tornadoes, respectively (Fig. 7). This increase in probability with an increase in parameter value, more steeply sloped for significant tornadoes compared with weak tornadoes, highlights the utility of STP in tornado forecasting. Furthermore, such distributions can be used as direct input to probabilistic tornado forecasting given environmental information near thunderstorms. Similar to effective bulk shear, a notable decline in conditional probabilities for significant tornadoes is evident for STP values of at least 12, though an attempt to explain this response physically is outside the scope of this work. Figure 7 also provides exceedance probabilities of tornadoes (weak and significant) corresponding to STP. Figure 7 suggests that exceedance probabilities increase with increasing STP, reinforcing the utility of STP as a parameter for assessing tornado potential. The increase in exceedance probabilities with increasing STP largely mirrors that for conditional probabilities, though the relatively large environs sample sizes play a role in muting conditional probabilities and exceedance probabilities.

Because of the substantial impact associated with significant tornadoes, a companion paper to this work (Hart and Cohen 2016, hereafter HC) specifically investigates significant tornado environments and their predictability as they vary seasonally. This motivates an experiment to investigate the validity of using the Bunkers et al. (2000) method for estimating storm motion within the context of the SSCRAM system. Given the established predictability of STP for significant

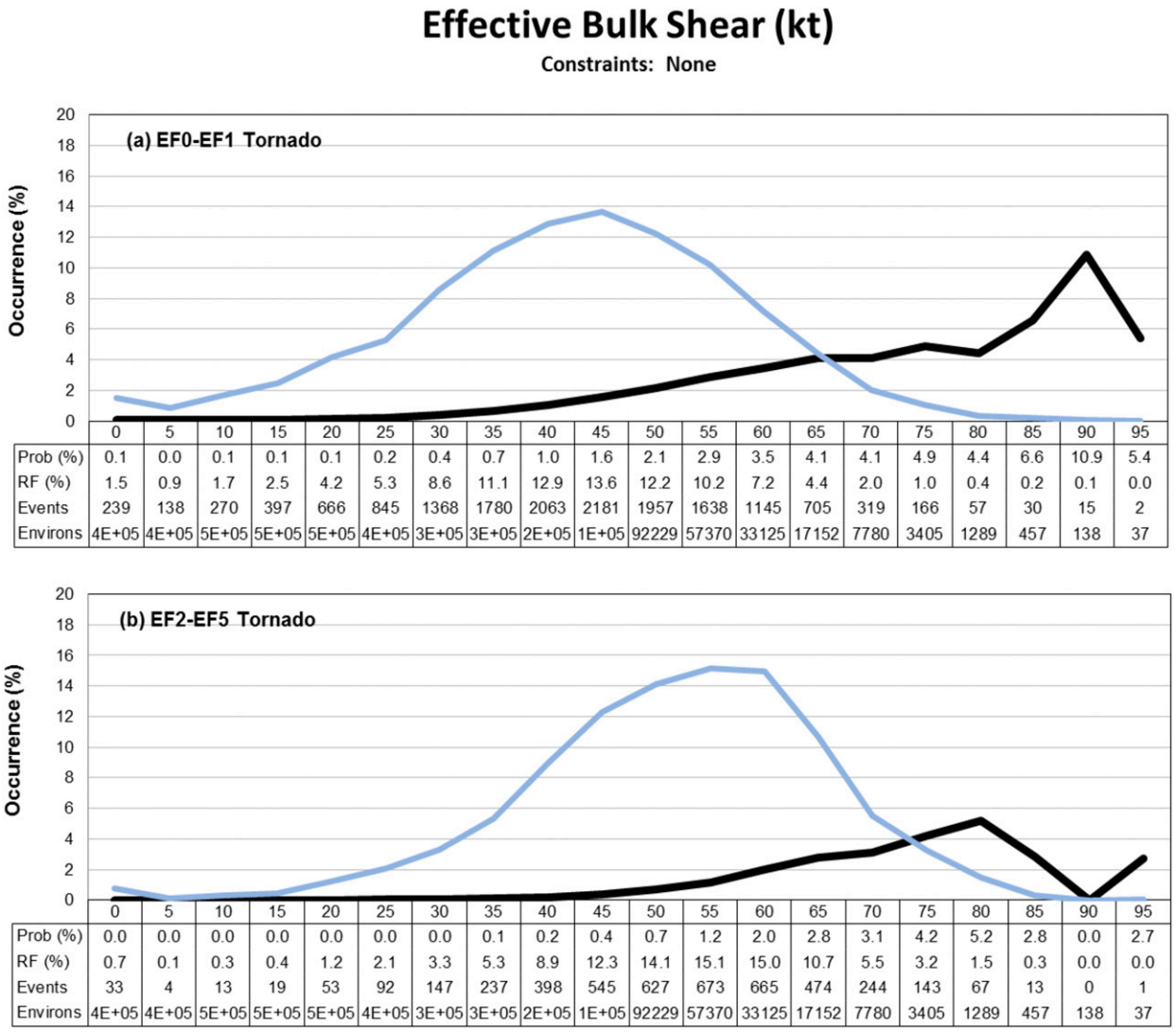

FIG. 6. The Prob (black) and RF (blue) plots for effective bulk shear corresponding to (a) weak and (b) significant tornado events. The plotting and labeling process follows Fig. 2.

tornado environments, we use this parameter as a proxy for comparing conditional probability distributions corresponding to four different methods of estimating storm motion to test the sensitivity of the SSCRAM system to storm motion estimates: the Bunkers et al. (2000) method, the Bunkers et al. (2014) method, the 30R75 method (storm motion is estimated to be to the right of the mean wind by 30° with a magnitude of 75% of mean wind speed) as described by Maddox (1976), and the 0–6-km pressure-weighted mean wind. This is done specifically for the subset of the SSCRAM dataset corresponding to the year 2011.

The results of this sensitivity analysis are presented in Fig. 8, which illustrates relatively similar variability in conditional probabilities with varying parameter ranges among the four storm motion estimates for significant tornadoes in 2011. Differences in conditional probabilities using STP among the four methods are all within around 10%, and this is the case when using effective bulk shear, MUCAPE, and STP for developing conditional probabilities for any type of severe weather reports in 2011 (not shown). However, Fig. 8 displays a consistent signal for conditional probabilities associated with the Bunkers et al. (2000) (and Bunkers et al. 2014) technique to match or exceed those corresponding to other storm motion estimates while maintaining the same structural pattern in the conditional probability distribution across the plotted ranges of STP values. This suggests that the Bunkers et al. (2000) method is an

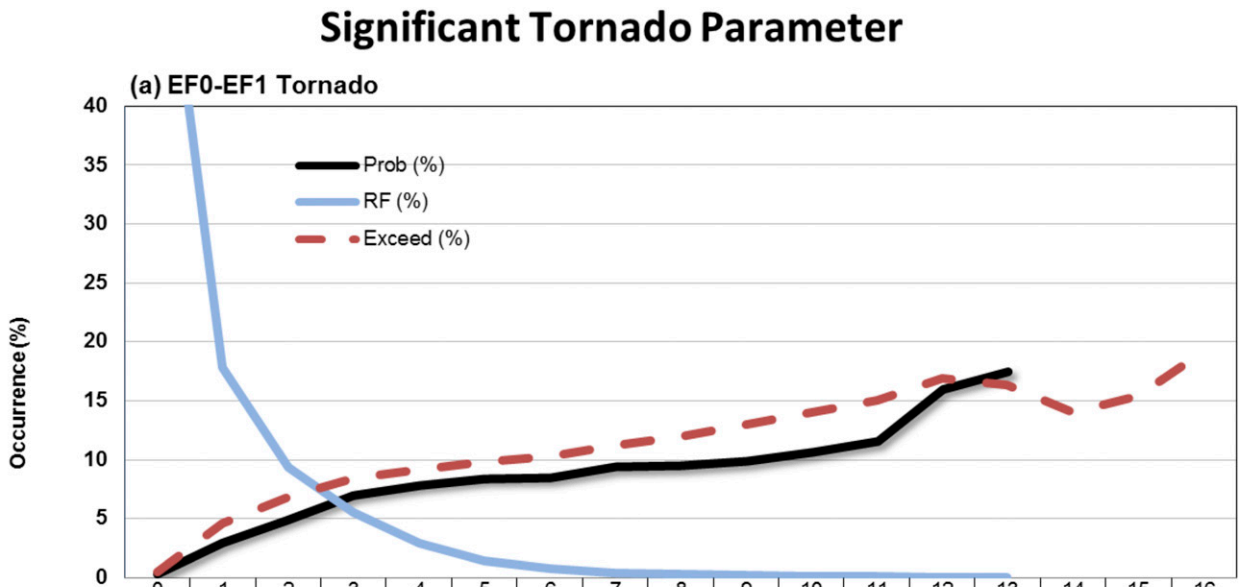

	0	1	2	3	4	5	6	7	8	9	10	11	12	13	14	15	16
Prob (%)	0.3	3.0	4.9	7.0	7.8	8.4	8.4	9.3	9.4	9.8	10.6	11.5	15.9	17.4			
RF (%)	60.7	17.9	9.4	5.6	2.9	1.4	0.8	0.5	0.3	0.2	0.1	0.1	0.1	0.1			
Events	9687	2853	1498	887	469	231	120	72	48	29	18	14	11	8			
Environs	4E+06	96427	30340	12709	5997	2755	1421	772	509	296	170	122	69	46			
Exceed (%)	0.5	4.6	6.8	8.4	9.2	9.8	10.3	11.2	12.0	13.0	14.0	15.0	16.9	16.3	14.0	15.4	19.2

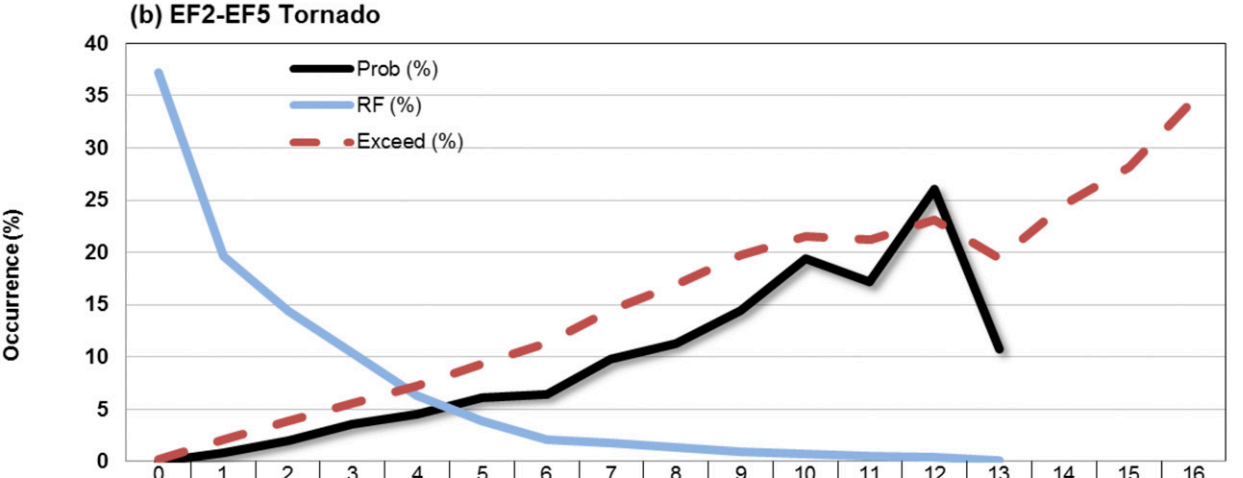

	0	1	2	3	4	5	6	7	8	9	10	11	12	13	14	15	16
Prob (%)	0.0	0.9	2.1	3.6	4.7	6.2	6.5	9.8	11.4	14.5	19.4	17.2	26.1	10.9			
RF (%)	37.2	19.7	14.4	10.4	6.3	3.9	2.1	1.7	1.3	1.0	0.7	0.5	0.4	0.1			
Events	1652	874	640	462	280	171	93	76	58	43	33	21	18	5			
Environs	4E+06	96427	30340	12709	5997	2755	1421	772	509	296	170	122	69	46			
Exceed (%)	0.1	2.1	3.8	5.6	7.2	9.3	11.3	14.5	16.9	19.7	21.6	21.2	23.1	19.4	24.6	28.2	34.6

FIG. 7. The Prob (black) and RF (blue) plots for STP corresponding to (a) weak and (b) significant tornado events. The plotting and labeling process follows Fig. 2. Exceedance probabilities are overlaid, which correspond to the conditional probabilities of tornado occurrence based on STP of at least the value listed along the *x* axis.

appropriate method for estimating storm motions within the context of the SSCRAM system, which is specifically relevant for the companion paper (HC), as it most fully represents downstream significant-tornado reports compared to the other methods using STP. Furthermore, since the majority of tornadoes and significantly severe hail are associated with supercells, and no one particular convective mode explains an appreciable

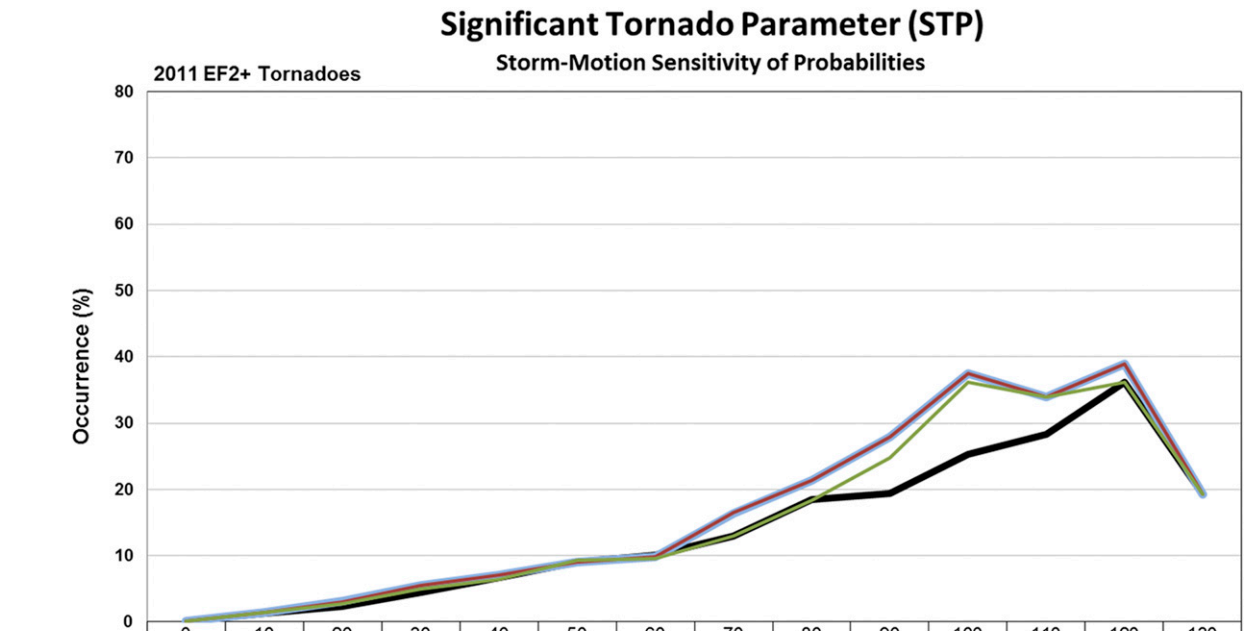

	0	10	20	30	40	50	60	70	80	90	100	110	120	130
Mean Wind	0.1	1.3	2.4	4.4	6.7	9.0	10.1	13.0	18.5	19.4	25.4	28.3	36.1	19.2
Bunkers	0.1	1.5	3.1	5.5	7.1	9.0	9.8	16.3	21.4	28.0	37.5	34.0	38.9	19.2
Eff Bunkers	0.1	1.4	3.1	5.6	7.1	9.0	9.9	16.5	21.4	28.0	37.5	34.0	38.9	19.2
30R75	0.1	1.5	2.8	4.9	6.4	9.3	9.6	13.0	18.3	24.7	36.1	34.0	36.1	19.2

FIG. 8. The Prob plots for STP overlaid corresponding to significant tornado events during 2011 using four different storm motions: pressure-weighted mean wind in the lowest 6 km above ground in black, the Bunkers et al. (2000) method in light blue, the Bunkers et al. (2014) method in dark red, and the 30R75 method in dark green. Probabilities of significant tornado occurrence corresponding to each of these overlaid plots are listed beneath the *x* axis.

proportion of significantly severe wind (Table 1 in Smith et al. 2012), the use of a supercell-based storm motion in SSCRAM provides a consistent method for characterizing storm motion for most high-impact severe weather hazards. However, solely basing storm motion on right-moving supercells does limit SSCRAM's utility in assessing storm motion accompanying severe hazards emanating from other convective modes.

While not shown, the use of 0–6-km pressure-weighted mean wind as a method for approximating storm motions in SSCRAM yields a more consistent representation of downstream severe storm reports compared to other methods and thus the highest conditional probabilities for any severe hazard type in 2011. Regardless, these conditional probability differences are small (generally within 10%) among the various methods. Furthermore, the establishment of a focus on significant tornado environments as the foundation for HC warrants the use of the Bunkers et al. (2000) method as a consistent storm-motion approximation in the SSCRAM system.

Other commonly used parameters in assessing tornado potential include LCL and SRH, with analyses for these parameters provided in Figs. 9 and 10, respectively, as the relationship between LCL height, SRH, and tornadoes has been often referenced in operational meteorology and tornado forecasting. For these two variables, LCL and SRH, additional constraints are placed on which grid points are analyzed for the purpose of limiting results to organized surface-based storms: effective bulk shear at least 50 kt, mixed-layer CAPE (MLCAPE) at least 1000 J kg^{-1}, and mixed-layer convective inhibition (MLCIN) of or smaller in magnitude than 50 J kg^{-1}. These particular constraints are based upon values relevant for anticipating organized, intense convection that the SPC is tasked with forecasting and specifically highlighting environments favoring the potential for surface-based supercells supporting the greatest tornado risk.

Using the aforementioned constraints to focus on environments of surface-based, organized convection, mixed-layer (lowest 100 mb) LCL (MLLCL) heights show a distinct signal for both weak and significant tornadoes to occur in environments with MLLCLs in the 500–1100-m range (Fig. 9). This finding alone is not inconsistent with previous notions that relatively low LCL heights are linked to tornado occurrence (Markowski et al. 2002). However, for individual ranges of MLLCL

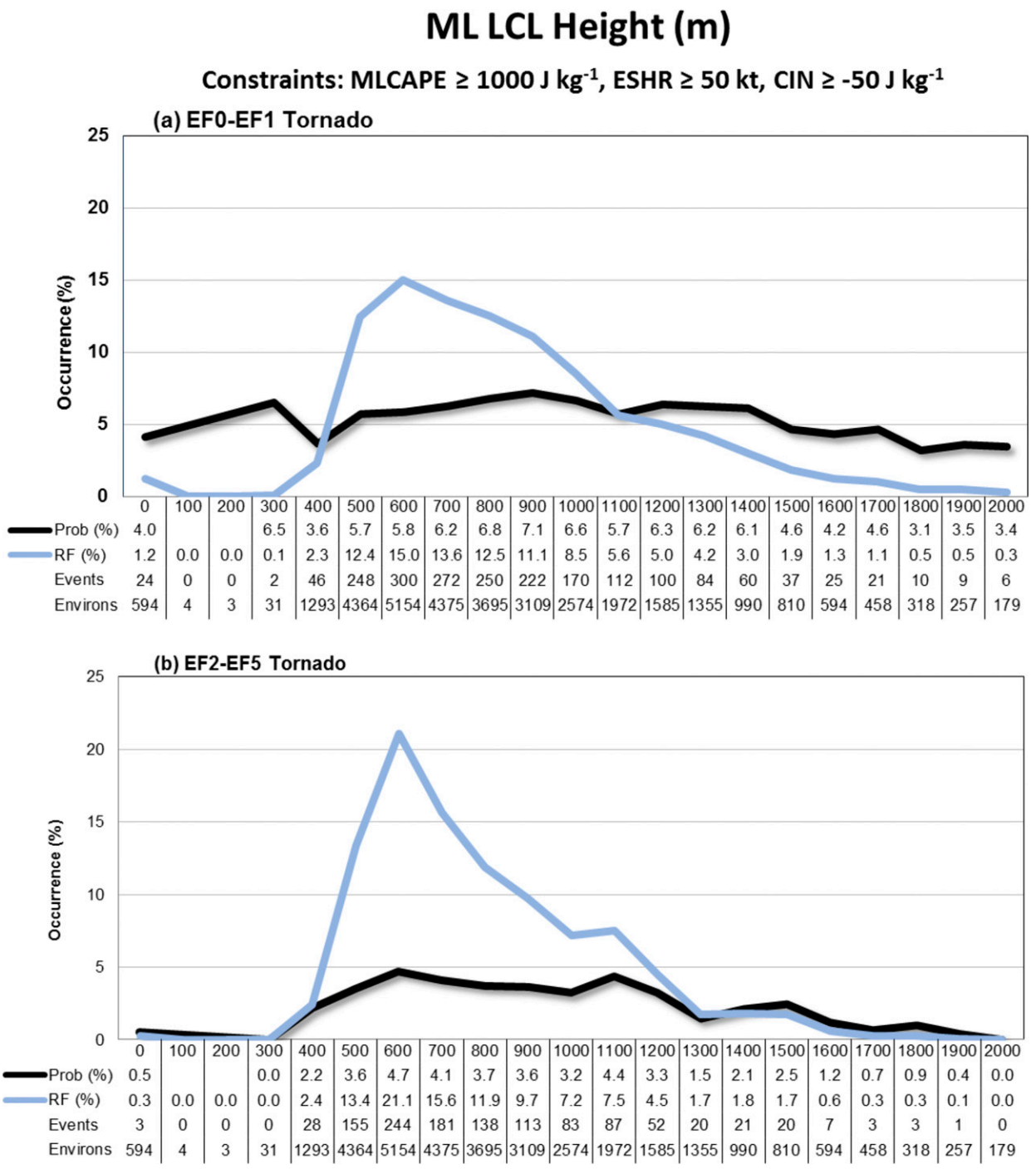

FIG. 9. The Prob (black) and RF (blue) plots for MLLCL (m AGL) corresponding to (a) weak and (b) significant tornado events. These plots use constraints for organized, surface-based convection: effective bulk shear at least 50 kt, MLCAPE at least 1000 J kg^{-1}, and MLCIN less negative than or equal to -50 J kg^{-1}.

height values, conditional probabilities of tornado occurrence are relatively small and uniform across the bulk of the tornado distribution and even outside of it, generally between 3% and 7% for weak tornadoes and slightly lower for significant tornadoes. This is a direct reflection of the notion that many environments supporting organized, surface-based convection that also have low MLLCLs do not result in downstream tornado

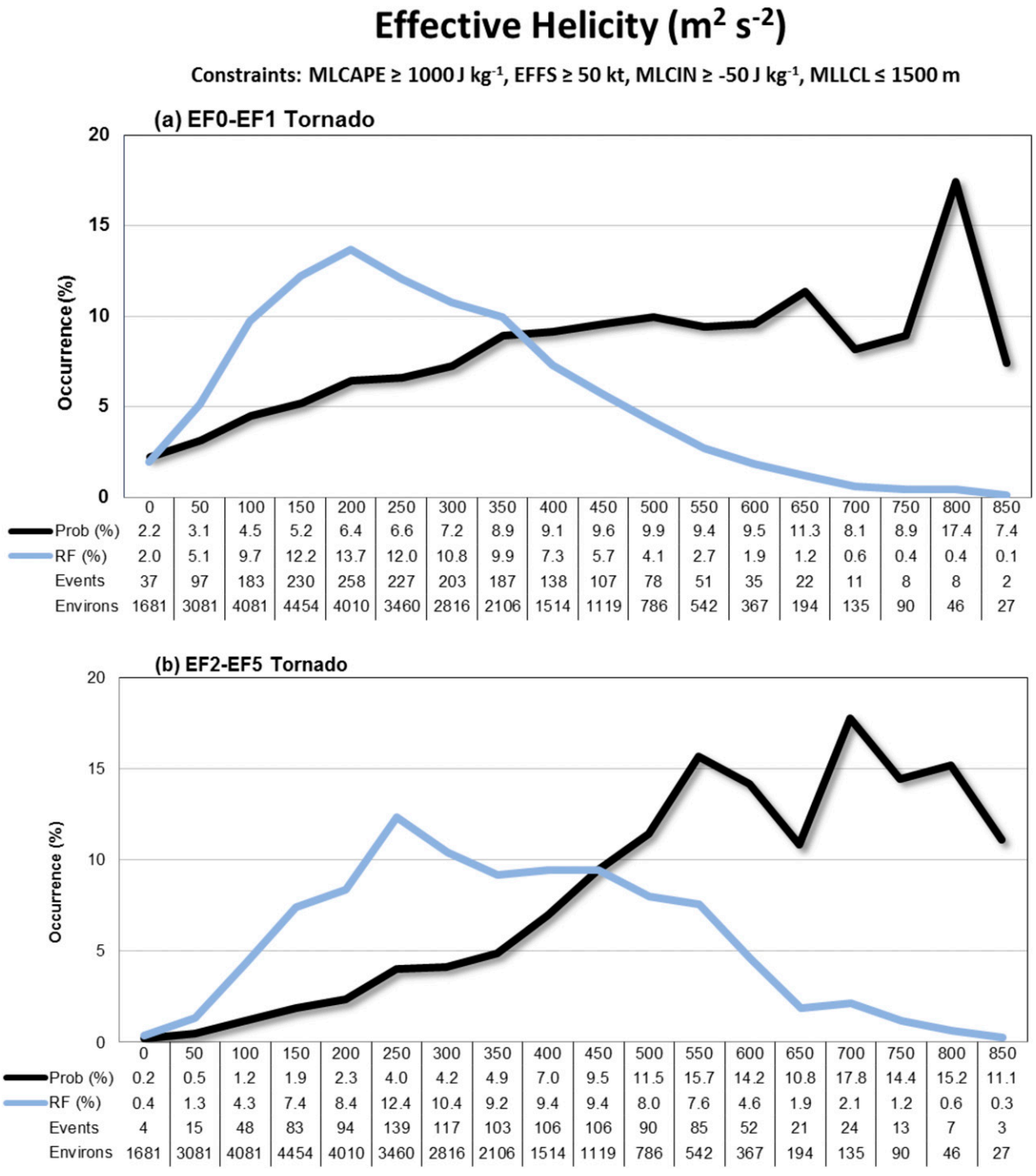

FIG. 10. The Prob (black) and RF (blue) plots for effective SRH ($m^2 s^{-2}$) corresponding to (a) weak and (b) significant tornado events. These plots use constraints for organized, surface-based convection: effective bulk shear at least 50 kt, MLCAPE at least 1000 J kg^{-1}, MLCIN less negative than or equal to -50 J kg^{-1}, and MLLCL at or below 1500 m.

occurrence when considered independently of other factors (e.g., SRH). The process of removing the constraints corresponding to organized, surface-based convection suggests little (not shown) overall difference from the application of these constraints in terms of expressing a uniformity of conditional probabilities using MLLCL as a tornado predictor. In discriminating between quasi-linear convective system tornadoes

producing ≥EF1 damage and right-moving supercell significant tornadoes, Thompson et al. (2012) indicated similarities among the distributions of MLLCL height during the spring, winter, and fall. The present study reflects a lack of predictive utility of this same parameter for values below 2000 m.

Considering the same constraints to focus on organized, surface-based convection, Fig. 10 indicates effective SRH for MLLCL heights below 1500 m, which represents the bulk of tornado-producing environments from Fig. 9. Effective SRH shows a more consistent signal for increasing tornado probability with increasing parameter value. Conditional probabilities for both weak and significant tornadoes reach or exceed around 10% at and above 500 $m^2 s^{-2}$ of effective SRH, and the probability curve experiences stronger positive slope for significant tornadoes than for weak tornadoes, especially around and above 300 $m^2 s^{-2}$. Figure 10 also highlights a skewed distribution in effective SRH for tornado occurrence, where proportions of tornadoes (weak and significant) gradually diminish with increasing SRH, suggesting a rarity for tornadoes occurring in association with effective SRH over 700 $m^2 s^{-2}$. Overall, these results suggest the necessity of incorporating effective SRH in quantitatively assessing tornado probability, more so than LCL height (Fig. 9), given the small probabilities and slight variability therein for tornado occurrence based on LCL height below 2000 m. Some of the fluctuations of conditional probabilities of tornadoes for relatively higher SRH are noted, but as with aforementioned fluctuations linked to effective bulk shear and STP, further analysis of these fluctuations are outside the scope of the present work, and small sample size could also play a role in explaining these fluctuations at the relatively higher SRH values.

4. Conclusions

The Statistical Severe Convective Risk Assessment Model (SSCRAM) is a system designed to associate all severe thunderstorm reports to mesoscale environmental information and is introduced in this paper. This system involves the consideration of environmental information of grid boxes featuring lightning, and subsequent downstream storm reports, using the Bunkers supercell motion technique as a proxy for storm motion. This affords us the opportunity to assess severe storm occurrences downstream of lightning strikes as a means to extend diagnostic mesoscale output to short-term, probabilistic output. For the present study, downstream severe storm reports are considered over a 2-h period beyond the top of the hour during which lightning occurred within a grid box, taking into account the forecast motion of the storm.

As a direct application of SSCRAM, conditional probabilities for severe storm events are assessed for five variables often considered in severe storms forecasting. Vertical shear—specifically, effective bulk shear—is found to offer greater utility in distinguishing between different probabilities of severe thunderstorm events compared to buoyancy. The effective-layer significant tornado parameter and effective storm-relative helicity are found to demonstrate a direct relationship between increasing parameter values and the conditional probability of downstream events, thus providing useful tornado probabilistic guidance, whereas lifting condensation level heights offer notably smaller and less-varying probabilities across most parameter values despite clustering in an optimal range for most tornado events. Ultimately, such work can feed directly into warn-on-forecast initiatives and other attempts to quantify severe storm occurrence based upon environmental information and the existence of a thunderstorm. Future work could investigate a wider array of convective evolutions and hazards (e.g., considering elevated versus surface-based convection, and significant versus nonsignificant severe wind and hail) and consider seasonal and regional variability in exploring the prognostic power of diagnostic parameters. In a companion paper, HC extend this work to evaluate the predictability of significant tornadoes during different times of the year.

Acknowledgments. The authors thank Andy Dean of the SPC for his help in accumulating severe thunderstorm reports and associated mesoanalysis environmental data, Jimmy Correia and Patrick Marsh for their ideas regarding the visualization of these data, and Israel Jirak for many insightful comments used to improve this manuscript, as well as many staff members of the SPC for their engaging discussion regarding interpretation of the results presented in this study. Valuable input from Richard Thompson was particularly appreciated in improving this manuscript. The authors also greatly appreciate Matthew Bunkers of the National Weather Service Forecast Office in Rapid City, South Dakota, along with two anonymous reviewers, for their feedback regarding this paper, which has greatly contributed to its improvement.

REFERENCES

Bothwell, P. D., J. A. Hart, and R. L. Thompson, 2002: An integrated three-dimensional objective analysis scheme in use at the Storm Prediction Center. Preprints, *21st Conf. on Severe Local Storms/19th Conf. on Weather Analysis and Forecasting/15th Conf. on Numerical Weather Prediction*, San Antonio, TX, Amer. Meteor. Soc., JP3.1. [Available online at https://ams.confex.com/ams/pdfpapers/47482.pdf.]

Bryan, G. H., J. C. Wyngaard, and J. M. Fritsch, 2003: Resolution requirements for the simulation of deep moist convection. *Mon. Wea. Rev.*, **131**, 2394–2416, doi:10.1175/1520-0493(2003)131<2394:RRFTSO>2.0.CO;2.

Bunkers, M. J., B. A. Klimowski, J. W. Zeitler, R. L. Thompson, and M. L. Weisman, 2000: Predicting supercell motion using a new hodograph technique. *Wea. Forecasting*, **15**, 61–79, doi:10.1175/1520-0434(2000)015<0061:PSMUAN>2.0.CO;2.

——, D. A. Barber, R. L. Thompson, R. Edwards, and J. Garner, 2014: Choosing a universal mean wind for supercell motion prediction. *J. Oper. Meteor.*, **2**, 115–129, doi:10.15191/nwajom.2014.0211.

Burgess, D. W., and L. R. Lemon, 1990: Severe thunderstorm detection by radar. *Radar in Meteorology*, D. Atlas, Ed., Amer. Meteor. Soc., 619–647.

Craven, J. P., and H. E. Brooks, 2004: Baseline climatology of sounding derived parameters associated with deep, moist convection. *Natl. Wea. Dig.*, **28**, 13–24.

Davies-Jones, R. P., D. Burgess, and M. Foster, 1990: Test of helicity as a forecasting parameter. Preprints, *16th Conf. on Severe Local Storms*, Kananaskis Park, AB, Canada, Amer. Meteor. Soc., 588–592.

Dean, A. R., R. S. Schneider, and J. T. Schaefer, 2006: Development of a comprehensive severe weather verification system at the Storm Prediction Center. Preprints, *23rd Conf. on Severe Local Storms*, St. Louis, MO, Amer. Meteor. Soc., P2.3. [Available online at https://ams.confex.com/ams/pdfpapers/115250.pdf.]

Done, J., C. A. Davis, and M. L. Weisman, 2004: The next generation of NWP: Explicit forecasts of convection using the Weather Research and Forecasting (WRF) model. *Atmos. Sci. Lett.*, **5**, 110–117, doi:10.1002/asl.72.

Doswell, C. A., III, and D. M. Schultz, 2006: On the use of indices and parameters in forecasting severe storms. *Electron. J. Severe Storms Meteor.*, **1** (3). [Available online at http://www.ejssm.org/ojs/index.php/ejssm/article/viewarticle/11/12.]

Edwards, R., R. L. Thompson, and J. A. Hart, 2002: Verification of supercell motion forecasting techniques. Preprints, *21st Conf. Severe Local Storms/19th Conf. on Weather Analysis and Forecasting/15th Conf. on Numerical Weather Prediction*, San Antonio, TX, Amer. Meteor. Soc., JP1.2. [Available online at https://ams.confex.com/ams/pdfpapers/46906.pdf.]

Galway, J. O., 1992: Early severe thunderstorm forecasting and research by the United States Weather Bureau. *Wea. Forecasting*, **7**, 564–587, doi:10.1175/1520-0434(1992)007<0564:ESTFAR>2.0.CO;2.

Hart, J. A., and A. E. Cohen, 2016: The challenge of forecasting significant tornadoes from June to October using convective parameters. *Wea. Forecasting*, doi:10.1175/WAF-D-16-0005.1, in press.

Jankov, I., and W. A. Gallus Jr., 2004: MCS rainfall forecast accuracy as a function of large-scale forcing. *Wea. Forecasting*, **19**, 428–439, doi:10.1175/1520-0434(2004)019<0428:MRFAAA>2.0.CO;2.

Johns, R. H., and C. A. Doswell III, 1992: Severe local storms forecasting. *Wea. Forecasting*, **7**, 588–612, doi:10.1175/1520-0434(1992)007<0588:SLSF>2.0.CO;2.

Kain, J. S., P. R. Janish, S. J. Weiss, M. E. Baldwin, R. S. Schneider, and H. E. Brooks, 2003: Collaboration between forecasters and research scientists at the NSSL and SPC: The Spring Program. *Bull. Amer. Meteor. Soc.*, **84**, 1797–1806, doi:10.1175/BAMS-84-12-1797.

Lewis, J., 1989: Realtime lightning data and its application in forecasting convective activity. Preprints, *12th Conf. on Weather Analysis and Forecasting*, Monterey, CA, Amer. Meteor. Soc., 97–102.

MacGorman, D. R., D. W. Burgess, W. D. Rust, W. L. Taylor, and B. C. Johnson, 1989: Lightning rates relative to tornadic storm evolution on 22 May 1981. *J. Atmos. Sci.*, **46**, 221–250, doi:10.1175/1520-0469(1989)046<0221:LRRTTS>2.0.CO;2.

Maddox, R. A., 1976: An evaluation of tornado proximity wind and stability data. *Mon. Wea. Rev.*, **104**, 133–142, doi:10.1175/1520-0493(1976)104<0133:AEOTPW>2.0.CO;2.

Maier, M. W., and E. P. Krider, 1982: A comparative study of cloud-to-ground lightning characteristics in Florida and Oklahoma thunderstorms. Preprints, *12th Conf. on Severe Local Storms*, San Antonio, TX, Amer. Meteor. Soc., 334–337.

Markowski, P. M., J. M. Straka, and E. N. Rasmussen, 2002: Direct surface thermodynamic observations within the rear-flank downdrafts of nontornadic and tornadic supercells. *Mon. Wea. Rev.*, **130**, 1692–1721, doi:10.1175/1520-0493(2002)130<1692:DSTOWT>2.0.CO;2.

Nag, A., and Coauthors, 2011: Evaluation of U.S. National Lightning Detection Network performance characteristics using rocket-triggered lightning data acquired in 2004–2009. *J. Geophys. Res.*, **116**, D02123, doi:10.1029/2010JD014929.

Rasmussen, E. N., and D. O. Blanchard, 1998: A baseline climatology of sounding-derived supercell and tornado forecast parameters. *Wea. Forecasting*, **13**, 1148–1164, doi:10.1175/1520-0434(1998)013<1148:ABCOSD>2.0.CO;2.

Rothfusz, L. P., E. Jacks, J. T. Ferree, G. J. Stumpf, and T. M. Smith, 2013: Next-generation warning concept: Forecasting a Continuum of Environmental Threats (FACETs). Preprints, *Second Conf. on Weather Warnings and Communication*, Nashville, TN, Amer. Meteor. Soc., 3.4. [Available online at https://ams.confex.com/ams/41BC2WxWarn/webprogram/Paper225900.html.]

Schneider, R. S., and A. R. Dean, 2008: A comprehensive 5-year severe storm environment climatology for the continental United States. Preprints, *24th Conf. on Severe Local Storms*, Savannah, GA, Amer. Meteor. Soc., 16A.4. [Available online at http://ams.confex.com/ams/pdfpapers/141748.pdf.]

Schultz, C. J., W. A. Petersen, and L. D. Carey, 2009: Preliminary development and evaluation of lightning jump algorithms for the real-time detection of severe weather. *J. Appl. Meteor. Climatol.*, **48**, 2543–2563, doi:10.1175/2009JAMC2237.1.

——, ——, and ——, 2011: Lightning and severe weather: A comparison between total and cloud-to-ground lightning trends. *Wea. Forecasting*, **26**, 744–755, doi:10.1175/WAF-D-10-05026.1.

——, L. D. Carey, E. V. Schultz, G. T. Stano, P. N. Gatlin, D. Kozlowski, R. J. Blakeslee, and S. J. Goodman, 2013: Integration of the total lightning jump algorithm into current operational warning environment conceptual models. Preprints, *Ninth Symp. on Future Operational Environmental Satellite Systems*, Austin, TX, Amer. Meteor. Soc., TJ30.4. [Available online at ams.confex.com/ams/93Annual/recordingredirect.cgi/id/24088.]

Schwartz, C. S., G. S. Romine, K. R. Smith, and M. L. Weisman, 2014: Characterizing and optimizing precipitation forecasts from a convection-permitting ensemble initialized by a mesoscale ensemble Kalman filter. *Wea. Forecasting*, **29**, 1295–1318, doi:10.1175/WAF-D-13-00145.1.

Scofield, R. A., and J. F. W. Purdom, 1986: The use of satellite data for mesoscale analyses and forecasting applications. *Mesoscale Meteorology and Forecasting*, P. S. Ray, Ed., Amer. Meteor. Soc., 118–150.

Smith, B. T., R. L. Thompson, J. S. Grams, C. Broyles, and H. E. Brooks, 2012: Convective modes for significant severe thunderstorms in the contiguous United States. Part I: Storm

classification and climatology. *Wea. Forecasting*, **27**, 1114–1135, doi:10.1175/WAF-D-11-00115.1.

Stensrud, D. J., and Coauthors, 2009: Convective-scale warn-on-forecast system: A vision for 2020. *Bull. Amer. Meteor. Soc.*, **90**, 1487–1499, doi:10.1175/2009BAMS2795.1.

Thompson, R. L., R. Edwards, J. A. Hart, K. L. Elmore, and P. Markowski, 2003: Close proximity soundings within supercell environments obtained from the Rapid Update Cycle. *Wea. Forecasting*, **18**, 1243–1261, doi:10.1175/1520-0434(2003)018<1243:CPSWSE>2.0.CO;2.

——, C. M. Mead, and R. Edwards, 2007: Effective storm-relative helicity and bulk shear in supercell thunderstorm environments. *Wea. Forecasting*, **22**, 102–115, doi:10.1175/WAF969.1.

——, B. T. Smith, J. S. Grams, A. R. Dean, and C. Broyles, 2012: Convective modes for significant severe thunderstorms in the contiguous United States. Part II: Supercell and QLCS tornado environments. *Wea. Forecasting*, **27**, 1136–1154, doi:10.1175/WAF-D-11-00116.1.

Trapp, R. J., S. A. Tessendorf, E. S. Godfrey, and H. E. Brooks, 2005: Tornadoes from squall lines and bow echoes. Part I: Climatological distribution. *Wea. Forecasting*, **20**, 23–34, doi:10.1175/WAF-835.1.

Weisman, M. L., C. Davis, W. Wang, K. W. Manning, and J. B. Klemp, 2008: Experiences with 0–36-h explicit convective forecasts with the WRF-ARW model. *Wea. Forecasting*, **23**, 407–437, doi:10.1175/2007WAF2007005.1.